E74-like ETS transcription factor 5 facilitates cell proliferation through regulating the expression of adenomatous polyposis coli 2 in non-small cell lung cancer

JING WEN[1,2*], GENGGENG QIN[1*], ZHAOJING JIANG[3*], ZIXUN LIN[2], RUIXIN ZHOU[2], HUI DAI[4], ZHANFA XU[1], WEIGUO CHEN[1] and QIANCHENG SONG[2,5]

[1]Department of Radiology, Nanfang Hospital, Southern Medical University; [2]Department of Cell Biology, School of Basic Medical Sciences, Southern Medical University, Guangzhou, Guangdong 510515; [3]Department of Radiation Oncology, Zhujiang Hospital, Southern Medical University, Guangzhou, Guangdong 510280; [4]Hospital Office, Ganzhou Hospital-Nanfang Hospital, Southern Medical University, Ganzhou, Jiangxi 341000; [5]Department of Neurosurgery, Institute of Brain Diseases, Nanfang Hospital, Southern Medical University, Guangzhou, Guangdong 510515, P.R. China

Received March 1, 2023; Accepted May 30, 2023

DOI: 10.3892/ijmm.2023.5278

Abstract. E74-like ETS transcription factor 5 (ELF5) is known to regulate the specification and differentiation of epithelial cells in the embryonic lung. However, the pathological function of ELF5 in lung cancer has yet to be fully elucidated. In the present study, the expression of ELF5 was found to be significantly higher in lung adenocarcinoma compared with that in corresponding adjacent normal tissues. Subsequently, cell and animal experiments were performed to investigate the role of ELF5 in lung adenocarcinoma cells. The results indicated that the overexpression of ELF5 increased the proliferation of lung adenocarcinoma cells, whereas, by contrast, a reduction in the expression of ELF5 led to a decrease in their proliferation. Mechanistically, the hypothesis is advanced that ELF5 can promote lung cancer cell proliferation through inhibiting adenomatous polyposis coli 2 and increasing the expression of cyclin D1, which is a critical downstream target of the Wnt pathway. Taken together, these findings support the notion that ELF5 exerts an essential role in the proliferation of lung adenocarcinoma cells and may be a therapeutic target for the treatment of lung adenocarcinoma.

Correspondence to: Professor Weiguo Chen, Department of Radiology, Nanfang Hospital, Southern Medical University, 1838 Guangzhou Avenue North Road, Baiyun, Guangzhou, Guangdong 510515, P.R. China
E-mail: chenweiguo1964@21cn.com

Professor Qiancheng Song, Department of Neurosurgery, Institute of Brain Diseases, Nanfang Hospital, Southern Medical University, 1838 Guangzhou Avenue North Road, Baiyun, Guangzhou, Guangdong 510515, P.R. China
E-mail: songqc@smu.edu.cn

*Contributed equally

Abbreviations: ELF5, E74-like ETS transcription factor 5; LLC, Lewis lung carcinoma; CCK-8, Cell Counting Kit-8; TMA tissue microarray; PCNA, proliferating cell nuclear antigen; RTCA, real-time cell analyzer; NSCLC, non-small cell lung cancer; APC2, adenomatous polyposis coli 2

Key words: lung adenocarcinoma, ELF5, proliferation

Introduction

E74-like ETS transcription factor 5 (ELF5), an ETS transcription factor, has been shown to be expressed in lung epithelial cells and to function as a crucial regulator of lung development (1,2). ELF5 regulates the specification and differentiation of epithelial cells in the fetal lung (1). ELF5 expression was also found to exhibit a dynamic expression pattern in the developing mouse lung, where its expression was restricted to distal epithelium during early development (1,2). By the end of the gestation period, ELF5 expression is enriched in proximal epithelial cells, although its expression is lost in the distal epithelium. Overexpression of ELF5 in the embryonic lung has been shown to disrupt branching morphogenesis, leading to a block in alveolar and airway differentiation (1).

An increasing body of evidence has revealed that ELF5 fulfills a tumor-suppressive role in prostate (3,4), bladder (5) and ovarian (6) cancer. It was found that ELF5 was lowly expressed in ovarian cancer tissues and highly expressed in adjacent tissues, indicating that the low expression of ELF5 may be closely associated with the occurrence of ovarian cancer (7). Both tumor-promoting and tumor-suppressive roles for ELF5 have been reported in breast cancer, and these differential functions may be linked to the subtype of the disease. ELF5 was reported to function as a tumor suppressor in basal and mesenchymal triple-negative breast cancer by preventing interferon-γ signaling-driven immunosuppressive alterations in the tumor microenvironment (8); nevertheless, another study demonstrated that an increased expression of ELF5 could drive metastasis and progression of estrogen receptor-positive (ER^+) breast cancer, rendering it resistant to endocrine therapy (9).

ELF5 is a key transcriptional effector in the lung (1,2); however, to the best of the authors' knowledge, the role of ELF5 in lung cancer has yet to be fully elucidated. Therefore, the aim of the present study was to investigate the role of ELF5 in lung cancer. It is shown that the expression of ELF5 in lung adenocarcinoma was significantly higher compared with that in corresponding adjacent normal tissues. Furthermore, an association was identified between ELF5 and lung adenocarcinoma growth both *in vitro* and *in vivo*, and ELF5 could promote the proliferation of lung adenocarcinoma cells. Mechanistically, adenomatous polyposis coli 2 (APC2) was found to be directly transcriptionally regulated by ELF5 during the regulation of lung cancer cells. Taken together, these findings provide new insights into the functions of ELF5, and its role in lung adenocarcinoma.

Materials and methods

Tissue microarray analysis. A human lung adenocarcinoma tissue microarray (cat. no. HLugA150CS03) that included 72 formalin-fixed, paraffin-embedded lung adenocarcinoma tissues and their corresponding adjacent lung tissues was randomly selected from the National Engineering Center for Biochip at Shanghai (Shanghai Outdo Biotech Co., Ltd.). The clinical characteristics of patients, including age, sex, histological grade and tumor-node-metastasis (TNM) stage, were obtained from the medical records of the patients, with certain missing clinical data excluded. Ethics approval (approval no. 81402373) was granted by the Human Research Ethics Committee of Taizhou Hospital of Zhejiang Province (Taizhou, China), and all patients or their next of kin provided their informed consent prior to the study. The present study was conducted in accordance with the principles and guidelines of The Declaration of Helsinki.

Immunohistochemical (IHC) analysis. Tissues were fixed in 4% paraformaldehyde at room temperature for 24 h or 10% formalin, embedded in paraffin, and 3-μm sections were cut for IHC analysis. Antigen retrieval was performed by boiling the tissue slices in sodium citrate buffer at 100˚C for 5 min. The activity of endogenous peroxide was blocked with 3% hydrogen peroxide for 10 min at room temperature, and 1% goat serum (cat. no. AR0009; Wuhan Boster Biological Technology, Ltd.) was applied to the sections at room temperature for 1 h as a blocking reagent to reduce non-specific binding. The ELF5 (1:100; cat. no. NHA6603; Novogene Co., Ltd.) and Ki-67 (1:200; cat. no. 9129S; Cell Signaling Technology, Inc.) antibodies were used as primary antibodies at 4˚C overnight, and subsequently the secondary antibody [goat anti-rabbit IgG (H+L)-HRP; cat. no. RM3002; Beijing Ray Antibody Biotech] was incubated with the tissue slices at room temperature for 1 h and stained with 3,3-diaminobenzidine (DAB) at room temperature for 2 min. After washing in phosphate-buffered saline (PBS) solution, the tissue slices were counterstained with conventional hematoxylin solution at room temperature for 2 min.

Each sample was evaluated and scored independently by two pathologists who were blinded to clinical, pathological and molecular data at the time of analysis. A total of two high-power visual fields were observed on each slice, and the IHC score was evaluated using a semi-quantitative method. Briefly, the scoring method was as follows: <1% positively stained cells was scored as 0; 1-30% positively stained cells was scored as 1; 31-60% positively stained cells was scored as 2; and >60% positively stained cells was scored as 3. Positive staining intensity was graded as follows: Colorless was scored as 0 (negative); light yellow was scored as 1 (weak); brown-yellow was scored as 2 (moderate); and brown was scored as 3 (strong). The two scores were multiplied to generate the IHC score (in the range 0-9). Positive expression of ELF5 was defined as the tissue having an IHC score ≥5. The images were acquired using an Olympus SZX16 stereomicroscope (Olympus Corporation) and analyzed using ZEN Imaging Software (version Zen 2011 Service Pack 1; Carl Zeiss AG).

Cell culture. The human lung adenocarcinoma cell line A549 (American Type Culture Collection), the murine Lewis lung carcinoma (LLC) (Procell Life Science & Technology Co., Ltd.) cell line and the human embryonic kidney cell line 293 (American Type Culture Collection) were cultured in DMEM with 10% Gibco® fetal bovine serum (Thermo Fisher Scientific, Inc.) and 1% Penicillin-Streptomycin (cat. no. 15140122; Gibco™; Thermo Fisher Scientific, Inc.). All cells were cultured in a 37˚C incubator with 5% CO_2 and 95% humidity. The cell lines were not authenticated after purchase, but routinely tested negative for mycoplasma contamination.

Plasmid construction and transfection. The open reading frame of ELF5 was amplified from 293 cells (American Type Culture Collection) cDNA and cloned into the pcDNA3.1 vector (Thermo Fisher Scientific, Inc.). The sequences were confirmed by Sanger sequencing. The recombinant plasmid and vector plasmid were transfected into A549 cells using Invitrogen® Lipofectamine 3000™ transfection reagent (Thermo Fisher Scientific, Inc.) at 37˚C for 6 h, following the manufacturer's protocol. The concentration of nucleic acid used was 500 ng/ml. At 48 h after transfection, the cells were collected for subsequent experiments.

Lentivirus infection. The 3rd generation of lentiviral packaging system was used to produce a lentivirus carrying the ELF5 shRNA. The lentivirus carrying the ELF5 shRNA was purchased from GeneCopoeia, Inc. The ELF5 small hairpin RNA (shRNA) (Table SI) was subcloned via a *Bam*HI-*Eco*RI restriction digest into a psi-LVRU6GP vector (GeneCopoeia, Inc.). The psi-LVRU6GP-scramble (GeneCopoeia, Inc.) was used as a control. The Calcium Phosphate Cell Transfection Kit (Beyotime Institute of Biotechnology) was used to co-transfect 5 μg of recombined lentiviral vectors with 3.75 μg of psPAX2 and 1.25 μg of pMD2 VSV-G packaging vectors in 293T cells (American Type Culture Collection) at 37˚C for 4 h. The culture supernatants were collected after 48 h after transfection. Following centrifugation to remove cell debris, the supernatant was filtered through 0.45-μm polyethersulfone low protein-binding filters. The virus stock was aliquoted and kept at -80˚C until use. A549 and LLC cells were transduced with the lentivirus containing the ELF5 shRNA at a multiplicity of infection (MOI) of 6. The nucleotide sequence is GCCCTG AGATACTACTATAAA (Table SI). Briefly, $2x10^5$ cells were seeded in each well of a 12-well plate and incubated at 37˚C

in an atmosphere of 5% CO_2 overnight. Subsequently, the cells were infected with either lentivirus containing the ELF5 shRNA or vector virus, respectively. After 24 h, the cell culture medium was replaced with fresh medium. Fresh medium containing puromycin was added, and the medium was replaced with fresh puromycin-containing media every 2 days.

Western blot analysis. Cells were lysed in buffer containing 1 mM phenylmethylsulfonylfluoride (PMSF), 1X phosphatase inhibitor and 1X protease inhibitor cocktail. Following centrifugation at 12,000 x g for 10 min at 4˚C, the protein concentration was determined using a BCA Protein Assay Kit (Thermo Fisher Scientific, Inc.), and total proteins (the mass of protein loaded per lane, ≥20 μg) were further analyzed using 10% SDS-PAGE. The samples were then transferred to a polyvinylidene difluoride membrane and 5% BSA was applied to the sections at room temperature for 1 h as a blocking reagent to reduce non-specific binding. The samples were then probed with antibodies against β-actin (1:4,000; cat. no. RM2001; Beijing Ray Antibody Biotech), ELF5 (1:500; cat. no. NHA1145; Novogene Co, Ltd.), proliferating cell nuclear antigen (PCNA) (1:1,500; cat. no. 13110; Cell Signaling Technology, Inc.), APC2 (1:500; cat. no. ab233753; Abcam) and cyclin D1 (1:1,000; cat. no. 55506; Cell Signaling Technology, Inc.). Following the incubation with primary antibodies at room temperature for 1 h, the membranes were washed with TBS/0.05% Tween-20 and incubated with HRP-conjugated secondary antibodies (1:3,000; cat. nos. RM3001 and RM3002; Beijing Ray Antibody Biotech) at room temperature for 1 h. Proteins were detected using enhanced chemiluminescence substrates (PerkinElmer, Inc.). The results were quantified using ImageJ software (version 1.52A; National Institutes of Health).

Cell Counting Kit-8 (CCK-8) assay. Cell proliferation was measured using CCK-8 assay. Briefly, 2,000 cells were plated into each well of a 96-well plate and incubated at 37˚C in an atmosphere containing 5% CO_2. Subsequently, 10 μl CCK-8 solution (Vazyme Biotech Co., Ltd.) was added to each well. The cells were then incubated for 2 h at 37˚C, and the absorbance was measured using a microplate reader at 450 nm. Three independent experiments were performed. The data were plotted in order to derive the cell proliferation curves.

Real-time cell proliferation assay. The proliferative ability of the cells was monitored using the xCELLigence R Real-Time Cell Analyzer S16 (RTCA S16) (ACEA Bioscience, Inc.). This platform is able to measure cellular growth status in real time. Briefly, 2,000 cells were plated into the special plate (E-Plate 16) per well. After a 30-min incubation, E-Plate 16 and the xCELLigence RTCA S16 system were connected for the purposes of scanning the plate. Cell growth was monitored continuously and recorded as a cell index. The whole device was placed in an incubator at 37˚C containing 5% CO_2 for 104 h. The cell index was derived from the change in electrical impedance as the living cells interacted with the biocompatible microelectrode surface in the microplate well, which provided an effective means of measuring the cell number. The cell index was read automatically, and the recorded curves are shown as the cell index ± SEM.

Animal studies. C57BL/6, five-week-old male mice (n=6, weight, 20±1.5 g) were purchased from The Animal Center of Southern Medical University (Guangzhou, China). All mice were housed in specific pathogen-free conditions in an environment with regulated temperature (22±1˚C) and humidity (40-70%) and exposure to a constant 12-h light-dark cycle in the animal facility. A total of $1x10^6$ LLC cells suspended in 100 μl saline were injected subcutaneously (and intraperitoneally) into the lateral thighs of the mice (n=6), and this operation was performed under anesthesia [60 mg/kg sodium pentobarbital (body weight)]. The cells were implanted on the right side for the control group, whereas for the ELF5-shRNA group, they were implanted on the left side. The size of the tumors was evaluated for the first time nine days after injection using calipers, according to the following formula: Tumor volume=(length x width^2)/2. The health and behavior of the animals were monitored every 2 days. No mice succumbed and there were no abnormal signs of humane endpoints over the course of the experiment. At 24 days after injection of the cells, the mice were sacrificed via cervical dislocation, and all tumors were identified to be <2,000 cm^3 in size. Following confirmation that the experimental animals had no heartbeat or had ceased breathing, the tumors were isolated and weighed. The humane endpoints for the experiment were designated as follows: A marked reduction in food or water intake, labored breathing, an inability to stand and no response to external stimuli; however, no abnormal signs that were indicative of the humane endpoints of the experiment were observed in any of the mice during these experiments. All mouse experiments lasted one month and included acclimatization to the feeding environment, tumor implantation and growth, which were performed in compliance with the Institutional Animal Care and Use Committee guidelines of Southern Medical University, Guangzhou, China [approval no. SYXK (Guangdong) 2016-0167].

Promoter activity assay. Transfections and dual luciferase reporter assays were performed as previously described (10). Briefly, human genomic DNA was used as a template to amplify the mice APC2 fragments covering ~2 kb of the 5'-flanking sequence by PCR. Subsequently, the PCR products were inserted into the pGL3.0 basic vector (Promega Corporation), and their efficient insertion was confirmed by sequencing. To detect the potential binding sites, different constructs of mutated seed sequences for ELF5-binding sites in the promoter regions of the APC2 were cloned. For the luciferase reporter assay, 293T cells were cultured in 24-well plates and each well was transfected with 0.5 μg firefly luciferase reporter plasmid, 0.05 μg pRL-CMV plasmid (Promega Corporation) and 0.5 μg control or Flag-ELF5 construct using Invitrogen™ Lipofectamine 3000 (Thermo Fisher Scientific, Inc.). Luciferase activities were measured at 36 h following transfection using luciferase assay kits (Promega Corporation).

RNA sequencing (RNA-seq) and data processing. Total amounts and integrity of RNA which was extracted from cells using the TRIzol Lysis Reagent (cat. no. 10296028; Invitrogen; Thermo Fisher Scientific, Inc.) according to the user guidelines, were assessed using the RNA Nano 6000 Assay kit (cat. no. 5067-1511; Agilent Technologies, Inc.) of the Bioanalyzer

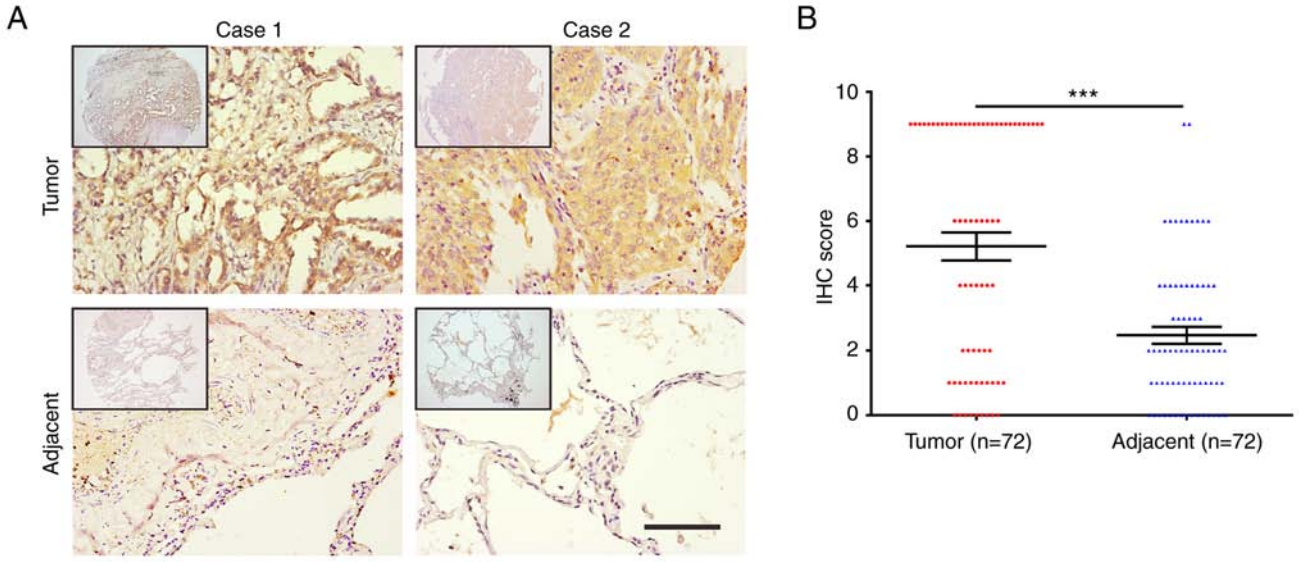

Figure 1. Expression of ELF5 in lung adenocarcinoma and corresponding adjacent normal tissues. (A) Representative images of the immunohistochemical analysis of ELF5 in lung adenocarcinoma and the corresponding adjacent normal tissues are demonstrated, based on the tissue microarray analysis (scale bars represent 100 μm). (B) The expression of ELF5 was significantly increased in lung adenocarcinoma compared with the corresponding adjacent normal tissues (n=72). Data were analyzed using the Chi-square test (***P<0.001). ELF5, E74-like ETS transcription factor 5.

2100 system (Agilent Technologies, Inc.). Briefly, mRNA was purified from total RNA using poly-T oligo-attached magnetic beads (cat. no. S1419S; New England BioLabs, Inc.). Second strand cDNA synthesis was subsequently performed using DNA Polymerase I and dNTP (cat. nos. M0210L and N0447L, respectively; New England BioLabs, Inc.). PCR amplification was then performed. The PCR product was purified using AMPure XP beads (cat. no. A63882; Beckman Coulter, Inc.), and the library was finally obtained. Following the construction of the library, reverse transcription-quantitative (RT-q) PCR was used to accurately quantify the effective concentration of the library (the effective concentration of the library was >2 nM) to ensure the quality of the library. After the library was qualified, it was sequenced using the Illumina NovaSeq 6000 (cat. no. 20012850; Illumina, Inc.). To generate the end reading of 150 bp. The basic principle of sequencing was to synthesize and sequence concurrently (sequencing by synthesis). Differential expression analysis of two conditions was performed using the edgeR package (3.22.5; https://bioconductor.org/packages/release/bioc/html/edgeR.html).

RT-qPCR analysis. Total RNA from cell lines was isolated using Life Technologies® TRIzol® reagent (Thermo Fisher Scientific, Inc.), according to the manufacturer's instructions. The reverse-transcription of RNA (2.0 μg) to cDNA was performed using the PrimeScript RT reagent kit (Takara Biotechnology Co., Ltd.) following the manufacturer's instructions. For the qPCR analysis, SYBR Green qPCR master mix (Takara Biotechnology Co., Ltd.) was used, following the protocol supplied by the manufacturer. The RT-qPCR thermocycling conditions were as follows: Initial denaturation at 95˚C for 30 sec, followed by 40 cycles at 95˚C for 5 sec and 60˚C for 20 sec. The $2^{-\Delta\Delta Cq}$ method (11) was used for the semi-quantification of the target genes, with GAPDH as the internal reference compound. The sequences of the primers used for qPCR are shown in Table SII.

Statistical analysis. Statistical analyses were performed using SPSS 20.0 software (IBM Corp.). All experiments were repeated at least three times and quantitative data were expressed as the mean ± standard error.Unpaired Student's t-test was used to compare means between groups. Chi-squared test was used to analyze the association between ELF5 expression and the clinicopathological parameters. P<0.05 was considered to indicate a statistically significant difference.

Results

ELF5 expression in lung adenocarcinoma is significantly higher compared with that in adjacent normal tissues. To identify the role of ELF5 in lung adenocarcinoma, the association between ELF5 expression and clinicopathological features in patients with lung adenocarcinoma based on the results from the tissue microarray (TMA) analysis was first retrospectively assessed (Fig. 1A and Table SII). Since ELF5 is a nuclear transcription factor, the evaluation of ELF5 expression was based exclusively on distinct nuclear staining intensity, through examining its staining rate in the nucleus (Fig. 1B). The results indicated that the ELF5 expression in lung adenocarcinoma was significantly higher compared with that in corresponding adjacent lung tissues. The association between the expression of ELF5 and the pathological characteristics of patients with lung adenocarcinoma was subsequently analyzed using the chi-square test. The results obtained revealed that the high expression of ELF5 was positively associated with stage classification and lymph node metastasis, but not with other pathological characteristics (Table SIII). Taken together, these results suggested that a strong association exists between ELF5 and lung adenocarcinoma growth.

ELF5 promotes the proliferation of lung adenocarcinoma cells. Subsequently, A549 cells were engineered to stably express the shRNA of ELF5 by infection of lentivirus with

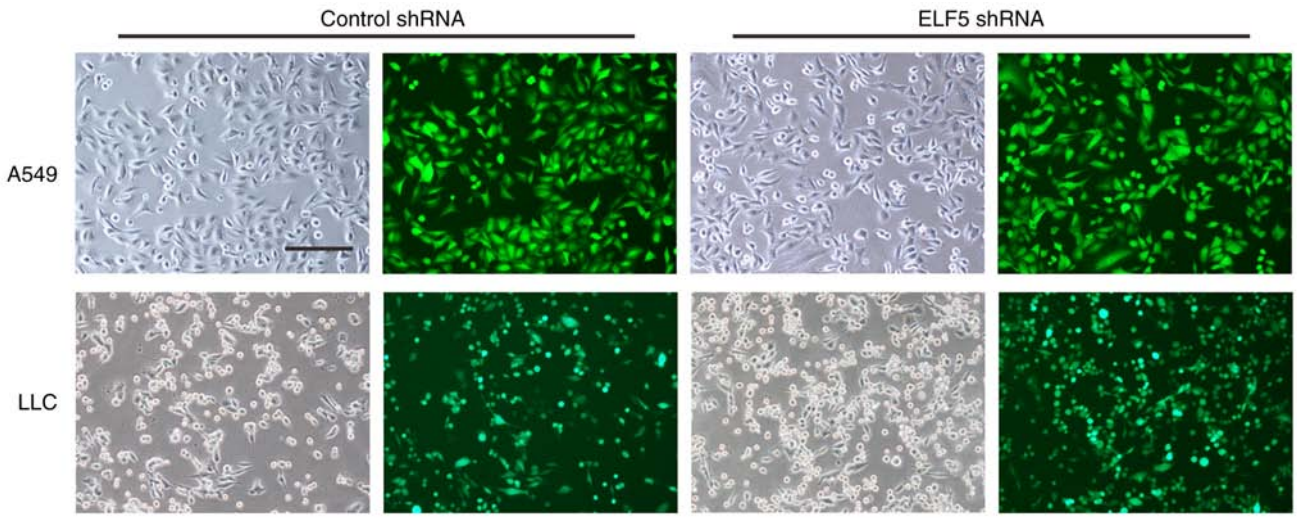

Figure 2. Lung adenocarcinoma cells engineered to stably express the shRNA of ELF5 through the infection of lentivirus with GFP fluorescence. After infecting A549 and LLC cells with lentivirus (ELF5 shRNA), the fluorescence intensity of EGFP was observed (scale bars represent 100 μm). ELF5, E74-like ETS transcription factor 5.

GFP fluorescence (Fig. 2). In addition, to identify the role of ELF5 in lung adenocarcinoma growth, lung adenocarcinoma A549 cells were transfected with pcDNA 3.1-ELF5 or the vector plasmid. Western blot analysis was employed to confirm the overexpression of ELF5 in A549 cells following transfection with pcDNA 3.1-ELF5 (Fig. 3A). Furthermore, the overexpression of ELF5 increased the expression of PCNA (Fig. 3A), a marker of cell proliferation that is commonly used to assess the growth fraction of a cell population (12,13). As shown in Fig. 3B and C, the overexpression of ELF5 led to an increase in the proliferation of A549 cells.

The results of western blot analysis verified a significant reduction of ELF5 in A549 cells following lentivirus infection (Fig. 3D). Furthermore, the low expression of ELF5 led to a decrease in the expression of PCNA. The proliferation of A549 cells was measured using CCK-8 assay (Fig. 3E) and the RTCA S16 system (Fig. 3F). The results showed that knocking down ELF5 significantly blocked the growth of A549 cells.

Knocked down expression of ELF5 decreases the proliferation of lung adenocarcinoma in vitro and in vivo. To further investigate the role of ELF5 in lung adenocarcinoma, mouse LLC cells were engineered to stably express the ELF5 shRNA via infection of lentivirus with green fluorescent protein (GFP) fluorescence (Fig. 2). Western blot analysis was used to confirm that a significant reduction in ELF5 expression in LLC cells occurred following lentivirus infection (Fig. 4A). Furthermore, the knocked down expression of ELF5 caused a decrease in the expression of PCNA. The proliferation of LLC cells was subsequently measured by CCK-8 assay (Fig. 4B) and the RTCA S16 system (Fig. 4C). The results obtained revealed that the reduction of ELF5 led to a decrease in the proliferation of LLC cells, findings that were consistent with those obtained in A549 cells.

Subsequently, an animal tumor model was constructed via the subcutaneous injection of LLC cells. The results obtained revealed that the knocked down expression of ELF5 led to a marked decrease in tumor growth *in vivo* (Fig. 4D and E). Subsequent IHC analysis of the tumor tissue showed that ELF5 knockdown led to a marked decrease in ELF5 levels in the tumor tissue (Fig. 4F). Moreover, the knocked down expression of ELF5 caused a decrease in the expression level of Ki-67, a commonly used marker of cell proliferation. Taken together, these results suggested that ELF5 is essential for lung adenocarcinoma cell growth.

APC2 acts as the direct target of ELF5 in the regulation of lung cancer cells. To further explore the underlying mechanism of ELF5 in lung cancer cells, RNA-Seq was performed following transfection of vector control or pcDNA3.1-ELF5 plasmid in LLC cells. A total of 323 DEGs, including 136 downregulated DEGs and 187 upregulated DEGs, were revealed in LLC cells following ELF5 overexpression (log2 |fold change|>1; P<0.05) (Fig. S1). A total of 6 DEGs were further confirmed using RT-qPCR analysis in LLC cells (Fig. 5A). Among these, APC2 was found to be involved in tumorigenesis, and was strongly suppressed by ELF5 overexpression.

In order to investigate the directly acting mechanism through which ELF5 promotes the proliferation of lung adenocarcinoma cells, JASPAR 2022 (14) was employed to predict APC2 as one of the downstream target genes of ELF5 (Fig. 5B). Subsequently, luciferase reporter assays were performed to validate that ELF5 could directly target the promoter of APC2. Through the transfection of wild-type (WT) or mutant (M1 or M2; i.e., mutations of the ELF5 binding sites) APC2 promoter reporter constructs into control or ELF5-overexpressed cells, ELF5 overexpression was revealed to significantly suppress the luciferase activity of the WT APC2 promoter reporter constructs compared to the vector, whereas the M1 or M1 + M2 constructs resulted in an increase in luciferase activity compared with that in the wild-type (Fig. 5C). These findings clearly demonstrated that ELF5 supresses the transcription of APC2 through the ELF5-binding site motifs. Western blot analysis revealed that overexpression of ELF5 led to a marked decrease in APC2 expression in lung adenocarcinoma cells, whereas the silencing of ELF5 resulted in an increase in APC2

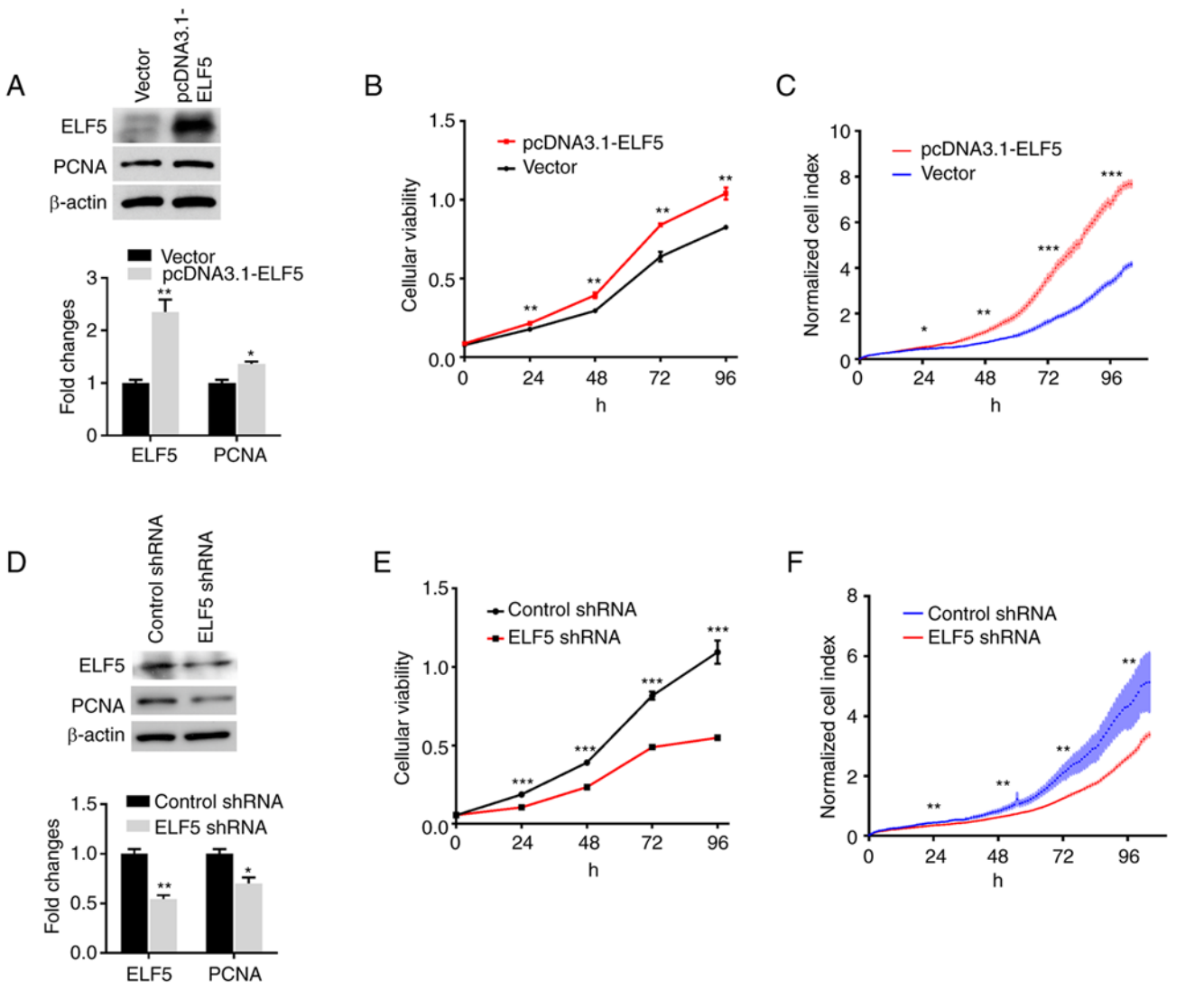

Figure 3. ELF5 promotes the proliferation of lung adenocarcinoma cells. A549 cells were transfected with either pcDNA 3.1-ELF5 or the control vector. (A) The expression of ELF5 and PCNA was detected using western blot analysis in A549 cells with β-actin serving as a loading control. The proliferation of A549 cells was assessed using (B) CCK-8 assay and (C) the RTCA S16 system. Subsequently, A549 cells were engineered to stably express the shRNA of ELF5 through the infection of lentivirus with GFP fluorescence. (D) The expression of ELF5 and PCNA was detected using western blot analysis in A549 cells with β-actin serving as a loading control. The proliferation of A549 cells was assessed using (E) CCK-8 assay and (F) the RTCA S16 system. The data were analyzed using unpaired t-test (*P<0.05, **P<0.01 and ***P<0.001). ELF5, E74-like ETS transcription factor 5; PCNA, proliferating cell nuclear antigen; CCK-8, Cell Counting Kit-8; RTCA S16, Real-Time Cell Analyzer S16.

expression (Fig. 5D and E). Furthermore, the results obtained demonstrated that ELF5 could increase cyclin D1 expression, and silencing of ELF5 caused a decrease in cyclin D1 expression in lung adenocarcinoma cells (Fig. 5D and E).

Discussion

Lung cancer is one of the leading causes of cancer-associated mortality globally (15,16). Non-small cell lung cancer (NSCLC) is the prominent type of lung cancer, which accounts for >80% of all cases of lung cancer. Despite some advances that have been made in terms of early detection of the tumor, and recent improvements in treatment, lung cancer remains a significant cause of both the mortality and morbidity of patients with cancer. Therefore, there is an urgent need to elucidate the molecular mechanisms underlying lung cancer progression, and to develop efficient therapies against lung cancer.

ELF5 was initially found to be expressed predominantly in epithelial cells, and it was shown to function as a crucial regulator of mammary gland development and milk production (17,18). During the course of normal breast development, ELF5 drives a cell fate decision of the mammary progenitor cells, causing them to establish the estrogen receptor-negative (ER^{-}) cell lineage responsible for alveolar development and milk production (18). ELF5 can not only induce mammary gland tumor cell transformation from the luminal subtypes to basal-like subtypes, but it can also inhibit the cell phenotype, effectively leading to an increase in estrogen sensitivity in breast cancer (19). Both tumor-promoting and tumor-suppressive roles for ELF5 have been reported in breast cancer, which may be linked to the subtype of the disease. Mutations in ELF5 are relatively rare in human cancers (20). Missense mutations occur in melanoma, mesothelioma, uterine, stomach and colorectal cancers, which are predominantly non-recurring

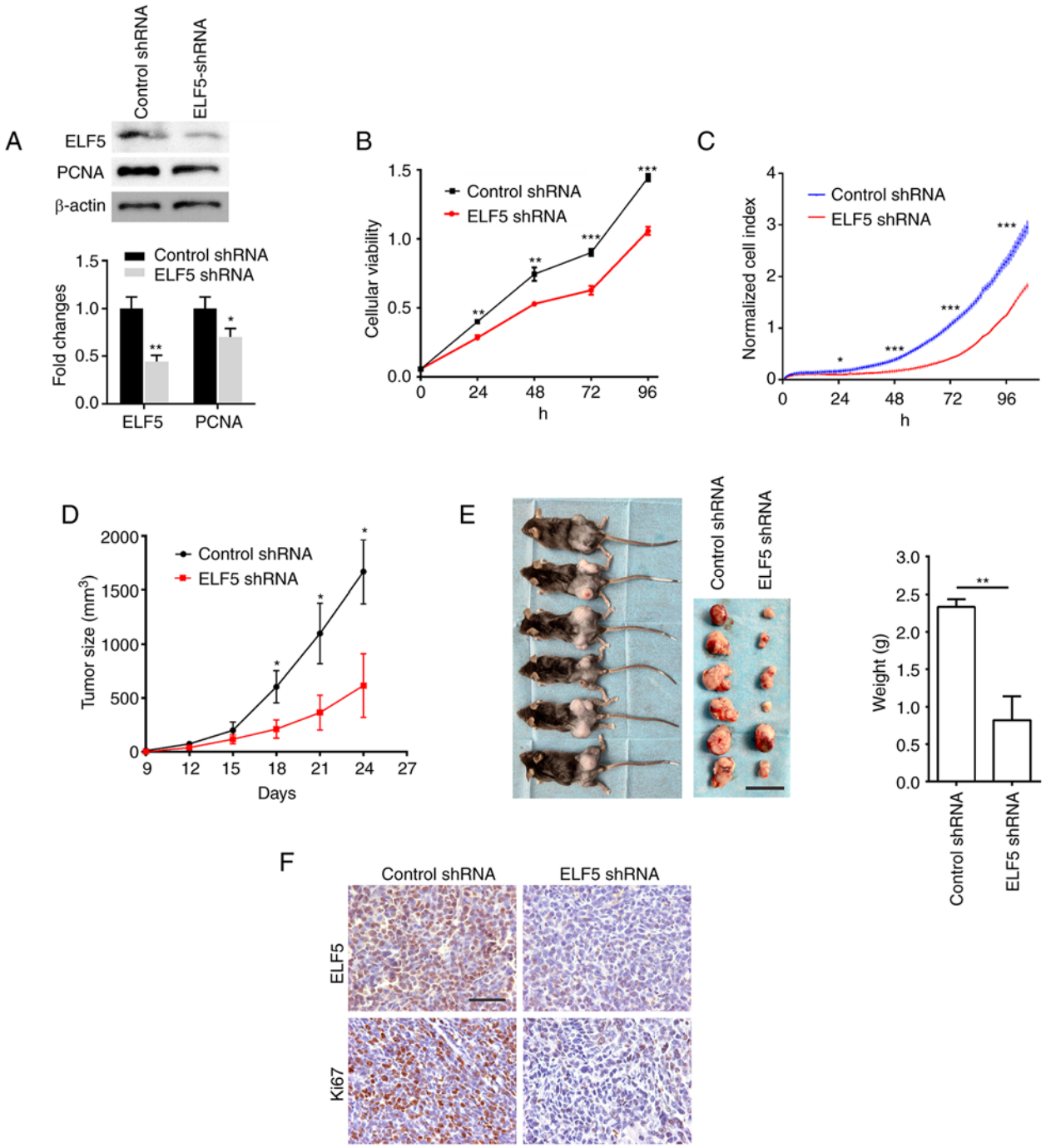

Figure 4. Knockdown of the expression of ELF5 decreases the proliferation of lung adenocarcinoma *in vitro* and *in vivo*. Mouse LLC cells were engineered to stably express the shRNA of ELF5 through infection of lentivirus with GFP fluorescence. (A) The expression of ELF5 and PCNA was detected using western blot analysis in LLC cells, with β-actin serving as a loading control. The proliferation of LLC cells was assessed using (B) Cell Counting Kit-8 assay and (C) the Real-Time Cell Analyzer S16 system. To construct the animal tumor model, $1x10^6$ LLC cells were subcutaneously injected into the lateral thigh of mice (n=6). (D) The size of the tumor was evaluated for the first time nine days after injection, and every 3 days thereafter, using calipers, according to the formula: Tumor volume=(length x width^2)/2. (E) After 24 days, the tumor tissue was isolated from the mice and weighed (scale bar, 20 mm). (F) The expression levels of ELF5 and Ki-67 in the tumor tissue were detected by immunohistochemical staining analysis (scale bars represent 100 μm). The data were analyzed using unpaired t-test (*P<0.05, **P<0.01 and ***P<0.001). ELF5, E74-like ETS transcription factor 5; LLC, Lewis lung cancer; PCNA, proliferating cell nuclear antigen.

missense mutations of unknown function. Amplification of ELF5 occurs in cancers of the upper gastrointestinal tract (esophageal and stomach), ovary, head and neck, and breast in 2-6% of cases, whereas occasional deletions of ELF5 occur in prostate, sarcoma, bladder, and lung cancers, as well as in acute myeloid leukemia and gliomas (20).

Although previous studies have assessed ELF5 in a variety of different cancer types (3-7), to the best of our knowledge there have been no studies published on determining the relevance of ELF5 in lung cancer tissues or its clinicopathological significance. In the present study, it was possible to determine that the expression of ELF5 in lung adenocarcinoma

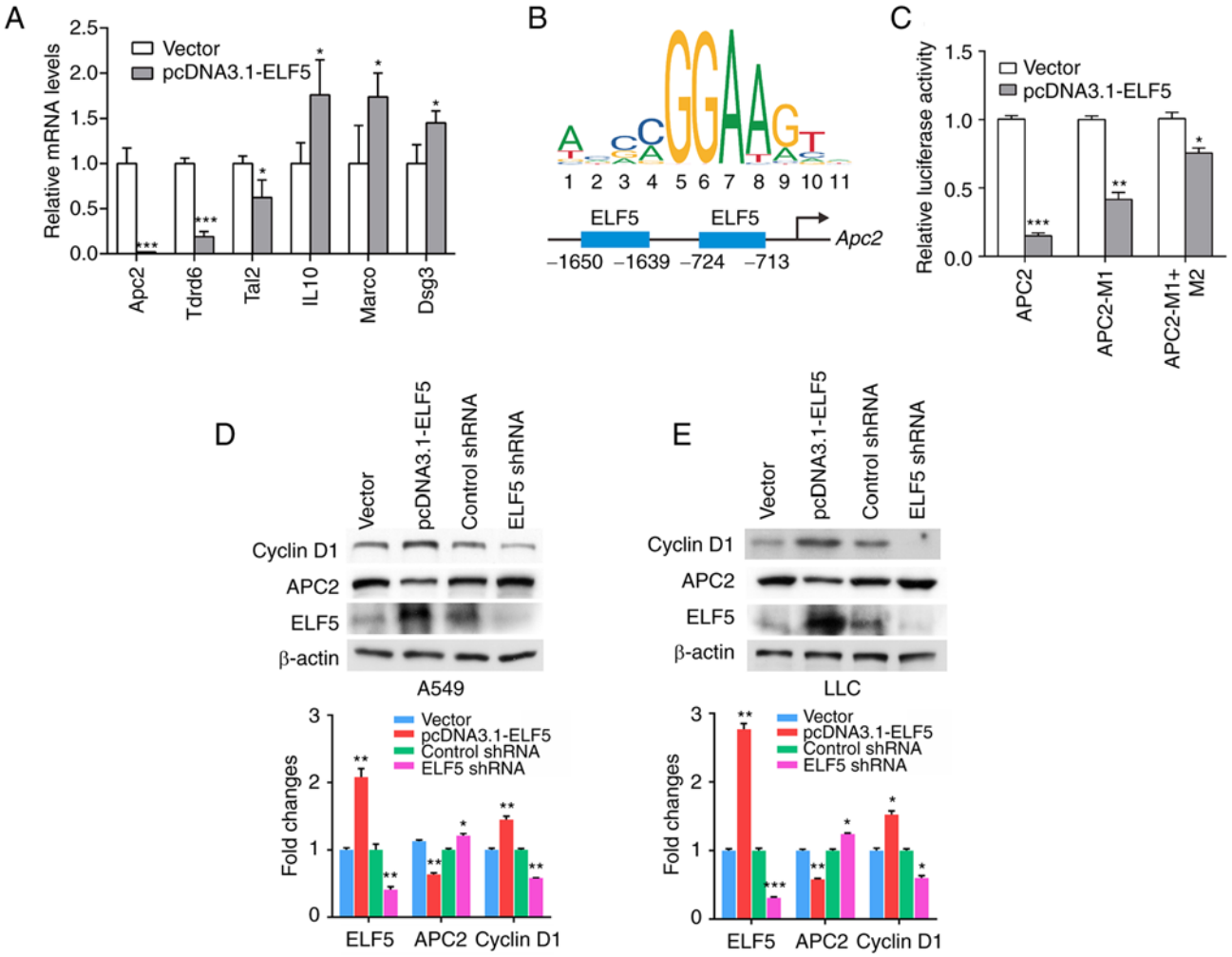

Figure 5. APC2 acts as the direct target of ELF5 in the regulation of lung cancer cells. (A) Reverse transcription-quantitative PCR analysis was performed, and the mRNA levels of 6 genes (Apc2, Tdrd6, Tal2, Il10, Marco and Dsg3) in LLC cells transfected with vector control or pcDNA3.1-ELF5 plasmid are shown (n=3; *P<0.05 and ***P<0.001). (B) ELF5 binding sites in the Apc2 promoter were predicted using JASPAR, and the binding sites are shown schematically in the diagrams. (C) Relative luciferase activity was detected in 293T cells that were co-transfected with pcDNA3.1-ELF5 plasmid or vector control and the wild-type Apc2 promoter or the mutated constructs (n=3; *P<0.05, **P<0.01 and ***P<0.001). Western blot analysis was performed, and the protein levels of cyclin D1, APC2 and ELF5 in (D) A549 cells and (E) LLC cells transfected with plasmid or infected with lentivirus containing the ELF5 shRNA are shown. *P<0.05, **P<0.01 and ***P<0.001. ELF5, E74-like ETS transcription factor 5; APC2, adenomatous polyposis coli 2.

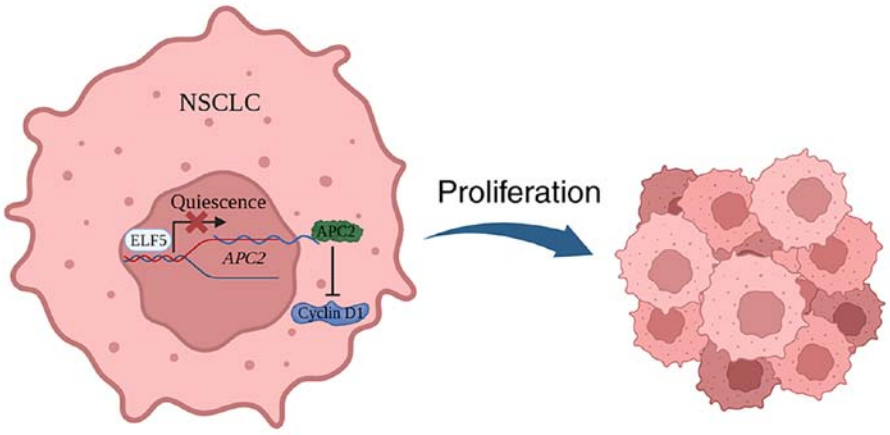

Figure 6. Schematic diagram showing the mechanistic role of E74-like ETS transcription factor 5 in the proliferation of non-small cell lung cancer. ELF, E74-like ETS transcription factor 5; NSCLC, non-small cell lung cancer; APC2, adenomatous polyposis coli 2.

was significantly higher compared with its expression in corresponding adjacent normal tissues, thereby suggesting that ELF5 may exert an important role in the development of lung adenocarcinoma. Due to the limited number of cases

in the present study, however, especially the number of lung adenocarcinoma patients with metastasis, the real prognostic significance of ELF5 remains to be elucidated in larger cohorts in lung adenocarcinoma.

In vitro experiments indicated that overexpression of ELF5 led to an increase in the proliferation of lung adenocarcinoma cells. On the other hand, a reduction in ELF5 expression led to a decrease in the proliferation of lung adenocarcinoma cells, showing that ELF5 was required for lung adenocarcinoma cell proliferation. Subsequent *in vivo* experiments showed that the low expression of ELF5 caused a marked decrease in tumor growth, a finding that was consistent with the experimental results identified *in vitro*. Therefore, these experiments revealed that ELF5 fulfills an essential role in the proliferation of lung adenocarcinoma cells.

APC2 has been shown to be closely associated with multiple aspects of lung development and lung tumor progression (21). The loss of APC2 has been observed previously in lung cancer (22), where it acts as a critical negative regulator of the Wnt signaling pathway (23,24). Downregulation of APC2 leads to the stabilization of active β-catenin, thereby increasing the activity of the Wnt pathway to promote lung cancer progression (23-26). In the present study, it was shown that ELF5 could promote lung cancer cell proliferation through inhibiting APC2. The mechanistic experiments revealed that ELF5 caused an increase in cyclin D1 expression, which is a critical downstream target of Wnt pathway (27,28), confirming that ELF5 could promote lung cancer cell proliferation through inhibiting APC2 and activating the Wnt pathway (Fig. 6).

Grainyhead-like 2 (GRHL2) plays multiple roles in lung morphogenesis that are essential for respiratory function (29-31). Loss of GRHL2 function in the lung epithelium of mice was shown to result in their death within hours of birth due to respiratory distress. Gene transcription profiling of GRHL2-deficient lung epithelial cells revealed a significant downregulation of ELF5. GRHL2 has been shown to control normal lung morphogenesis through tightly regulating the activity of distal tip progenitor cells through the direct regulation of ELF5 (30). GRHL2 has been implicated in tumor development in lung cancer, breast cancer, oral cancer and various gastric cancers (32,33). However, the function of GRHL2 appears to be complex and controversial in the context of cancer, varying with cancer type (34). GRHL2 was shown to be implicated as an oncogene in the etiology and progression of NSCLC (32). A higher level of GRHL2 expression in NSCLC is a predictor of poor prognosis. GRHL2 fulfills a regulatory role, participating in both cell proliferation and metastasis. GRHL2 was also shown to promote cell growth and colony formation, simultaneously suppressing the cell migration of NSCLC cells. Since ELF5 is regulated by GRHL2, GRHL2 may regulate the proliferation of lung cancer cells by regulating ELF5, although this aspect requires further study.

In conclusion, the findings of the present study have demonstrated that ELF5 exerts an essential role in the proliferation of lung adenocarcinoma cells. Furthermore, ELF5 was shown to promote lung cancer cell proliferation through inhibiting APC2. Taken together, the present study has shown that a higher expression level of ELF5 in lung adenocarcinoma may have potential as a therapeutic target option for the treatment of human lung adenocarcinoma.

Acknowledgements

Not applicable.

Funding

The present study was supported by the National Natural Science Foundation of China (grant no. 82202930), Tongling Science and Technology Project (grant no. 20200203037), the National Key Research and Development Program of China (grant no. 2019YFC0117301) and the Natural Science Foundation of Guangdong Province (grant no. 2019A1515011168).

Availability of data and materials

The datasets used and/or analyzed during the current study are available from the corresponding author on reasonable request. Data used for RNA-seq analysis in this study have been deposited into the Sequence Read Archive at the National Center for Biotechnology Information database under accession code PRJNA936676.

Authors' contributions

JW, GQ and ZJ contributed to the conceptualization, investigation, methodology, validation, and writing of the original draft. ZL, RZ, HD and ZX contributed to the formal analysis, visualization of the study and reviewing and editing. WC and QS contributed to the conceptualization, funding acquisition, resources, as well as the supervision of the study. All of the authors confirm the authenticity of all the raw data. All authors read and approved the final manuscript.

Ethics approval and consent to participate

The studies involving human tissue samples were approved (approval no. 81402373) by the Human Research Ethics Committee of Taizhou Hospital of Zhejiang Province (Taizhou, China), and all patients or their next of kin provided their informed consent prior to the study. The present study was conducted in accordance with the principles and guidelines of The Declaration of Helsinki. Animal experiments were conducted in accordance with the guidelines of the Institutional Animal Care and Use Committee of Southern Medical University, Guangzhou, China [approval no. SYXK (Guangdong) 2016-0167].

Patient consent for publication

Not applicable.

Competing interests

The authors declare that they have no competing interest.

References

1. Metzger DE, Stahlman MT and Shannon JM: Misexpression of ELF5 disrupts lung branching and inhibits epithelial differentiation. Dev Biol 320: 149-160, 2008.

2. Metzger DE, Xu Y and Shannon JM: Elf5 is an epithelium-specific, fibroblast growth factor-sensitive transcription factor in the embryonic lung. Dev Dyn 236: 1175-1192, 2007.
3. Yao B, Zhao J, Li Y, Li H, Hu Z, Pan P, Zhang Y, Du E, Liu R and Xu Y: Elf5 inhibits TGF-β-driven epithelial-mesenchymal transition in prostate cancer by repressing SMAD3 activation. Prostate 75: 872-882, 2015.
4. Li K, Guo Y, Yang X, Zhang Z, Zhang C and Xu Y: ELF5-mediated AR activation regulates prostate cancer progression. Sci Rep 7: 42759, 2017.
5. Wu B, Cao X, Liang X, Zhang X, Zhang W, Sun G and Wang D: Epigenetic regulation of Elf5 is associated with epithelial-mesenchymal transition in urothelial cancer. PLoS One 10: e0117510, 2015.
6. Yan H, Qiu L, Xie X, Yang H, Liu Y, Lin X and Huang H: ELF5 in epithelial ovarian carcinoma tissues and biological behavior in ovarian carcinoma cells. Oncol Rep 37: 1412-1418, 2017.
7. Hu Y, Yan Y, Xu Y, Yang H, Fang L, Liu Y, Li X, Li Q and Yan H: Expression and clinical significance of WWOX, Elf5, Snail1 and EMT related factors in epithelial ovarian cancer. Oncol Lett 19: 1281-1290, 2020.
8. Singh S, Kumar S, Srivastava RK, Nandi A, Thacker G, Muralil H, Kim S, Baldeon M, Tobias J, Blanco MA, *et al*: Loss of ELF5-FBXW7 stabilizes IFNGR1 to promote the growth and metastasis of triple-negative breast cancer through interferon-γ signalling. Nat Cell Biol 22: 591-602, 2020.
9. Piggin CL, Roden DL, Law AMK, Molloy MP, Krisp C, Swarbrick A, Naylor MJ, Kalyuga M, Kaplan W, Oakes SR, *et al*: ELF5 modulates the estrogen receptor cistrome in breast cancer. PLoS Genet 16: e1008531, 2020.
10. Yao F, Wang X, Cui ZK, Lan H, Ai X, Song Q, Chen Z, Yang J, Wu B and Bai X: ETS2 promotes epithelial-to-mesenchymal transition in renal fibrosis by targeting JUNB transcription. Lab Invest 100: 438-453, 2020.
11. Livak KJ and Schmittgen TD: Analysis of relative gene expression data using real-time quantitative PCR and the 2(-Delta Delta C(T)) method. Methods 25: 402-408, 2001.
12. Takasaki Y, Deng JS and Tan EM: A nuclear antigen associated with cell proliferation and blast transformation. J Exp Med 154: 1899-1909, 1981.
13. Juríková M, Danihel Ľ, Polák Š and Varga I: Ki67, PCNA, and MCM proteins: Markers of proliferation in the diagnosis of breast cancer. Acta Histochem 118: 544-552, 2016.
14. Castro-Mondragon JA, Riudavets-Puig R, Rauluseviciute I, Lemma RB, Turchi L, Blanc-Mathieu R, Lucas J, Boddie P, Khan A, Manosalva Pérez N, *et al*: JASPAR 2022: The 9th release of the open-access database of transcription factor binding profiles. Nucleic Acids Res 50 (D1): D165-D173, 2022.
15. Barta JA, Powell CA and Wisnivesky JP: Global epidemiology of lung cancer. Ann Glob Health 85: 8, 2019.
16. Bray F, Ferlay J, Soerjomataram I, Siegel RL, Torre LA and Jemal A: Global cancer statistics 2018: GLOBOCAN estimates of incidence and mortality worldwide for 36 cancers in 185 countries. CA Cancer J Clin 68: 394-424, 2018.
17. Zhou J, Chehab R, Tkalcevic J, Naylor MJ, Harris J, Wilson TJ, Tsao S, Tellis I, Zavarsek S, Xu D, *et al*: Elf5 is essential for early embryogenesis and mammary gland development during pregnancy and lactation. EMBO J 24: 635-644, 2005.
18. Oakes SR, Naylor MJ, Asselin-Labat ML, Blazek KD, Gardiner-Garden M, Hilton HN, Kazlauskas M, Pritchard MA, Chodosh LA, Pfeffer PL, *et al*: The Ets transcription factor Elf5 specifies mammary alveolar cell fate. Gene Dev 22: 581-586, 2008.
19. Kalyuga M, Gallego-Ortega D, Lee HJ, Roden DL, Cowley MJ, Caldon CE, Stone A, Allerdice SL, Valdes-Mora F, Launchbury R, *et al*: ELF5 suppresses estrogen sensitivity and underpins the acquisition of antiestrogen resistance in luminal breast cancer. PLoS Biol 10: e1001461, 2012.
20. Luk IY, Reehorst CM and Mariadason JM: ELF3, ELF5, EHF and SPDEF transcription factors in tissue homeostasis and cancer. Molecules 23: 2191, 2018.
21. Bonner AE, Lemon WJ, Devereux TR, Lubet RA and You M: Molecular profiling of mouse lung tumors: Association with tumor progression, lung development, and human lung adenocarcinomas. Oncogene 23: 1166-1176, 2004.
22. Miura K, Bowman ED, Simon R, Peng AC, Robles AI, Jones RT, Katagiri T, He P, Mizukami H, Charboneau L, *et al*: Laser capture microdissection and microarray expression analysis of lung adenocarcinoma reveals tobacco smoking- and prognosis-related molecular profiles. Cancer Res 62: 3244-3250, 2002.
23. Zhang K, Wang J, Yang L, Yuan YC, Tong TR, Wu J, Yun X, Bonner M, Pangeni R, Liu Z, *et al*: Targeting histone methyltransferase G9a inhibits growth and Wnt signaling pathway by epigenetically regulating HP1α and APC2 gene expression in non-small cell lung cancer. Mol Cancer 17: 153, 2018.
24. Croy HE, Fuller CN, Giannotti J, Robinson P, Foley AVA, Yamulla RJ, Cosgriff S, Greaves BD, von Kleeck RA, An HH, *et al*: The Poly(ADP-ribose) polymerase enzyme tankyrase antagonizes activity of the β-catenin destruction complex through ADP-ribosylation of axin and APC2. J Biol Chem 291: 12747-12760, 2016.
25. Dai B, Kong DL, Tian J, Liu TW, Zhou H and Wang ZF: microRNA-1205 promotes cell growth by targeting APC2 in lung adenocarcinoma. Eur Rev Med Pharmacol Sci 23: 1125-1133, 2019.
26. Dong Y, Wu B, Wang X, Lu F, Li Q and Zhao Q: High miR-3648 expression and low APC2 expression are associated with shorter survival and tumor progression in NSCLC. Histol Histopathol 37: 355-364, 2022.
27. Ge YX, Wang CH, Hu FY, Pan LX, Min J, Niu KY, Zhang L, Li J and Xu T: New advances of TMEM88 in cancer initiation and progression, with special emphasis on Wnt signaling pathway. J Cell Physiol 233: 79-87, 2018.
28. Rimerman RA, Gellert-Randleman A and Diehl JA: Wnt1 and MEK1 cooperate to promote cyclin D1 accumulation and cellular transformation. J Biol Chem 275: 14736-14742, 2000.
29. Varma S, Cao Y, Tagne JB, Lakshminarayanan M, Li J, Friedman TB, Morell RJ, Warburton D, Kotton DN and Ramirez MI: The transcription factors Grainyhead-like 2 and NK2-homeobox 1 form a regulatory loop that coordinates lung epithelial cell morphogenesis and differentiation. J Biol Chem 287: 37282-37295, 2012.
30. Kersbergen A, Best SA, Dworkin S, Ah-Cann C, de Vries ME, Asselin-Labat ML, Ritchie ME, Jane SM and Sutherland KD: Lung morphogenesis is orchestrated through Grainyhead-like 2 (Grhl2) transcriptional programs. Dev Biol 443: 1-9, 2018.
31. Gao X, Bali AS, Randell SH and Hogan BLM: GRHL2 coordinates regeneration of a polarized mucociliary epithelium from basal stem cells. J Cell Biol 211: 669-682, 2015.
32. Pan X, Zhang R, Xie C, Gan M, Yao S, Yao YB, Jin J, Han T, Huang Y, Gong Y, *et al*: GRHL2 suppresses tumor metastasis via regulation of transcriptional activity of RhoG in non-small cell lung cancer. Am J Transl Res 9: 4217-4226, 2017.
33. Werner S, Frey S, Riethdorf S, Schulze C, Alawi M, Kling L, Vafaizadeh V, Sauter G, Terracciano L, Schumacher U, *et al*: Dual roles of the transcription factor grainyhead-like 2 (GRHL2) in breast cancer. J Biol Chem 288: 22993-23008, 2013.
34. He J, Feng C, Zhu H, Wu S, Jin P and Xu T: Grainyhead-like 2 as a double-edged sword in development and cancer. Am J Transl Res 12: 310-331, 2020.